One Health 18 (2024) 100744

Contents lists available at ScienceDirect

One Health

journal homepage: www.elsevier.com/locate/onehlt

Susceptibility and transmissibility of SARS-CoV-2 variants in transgenic mice expressing the cat angiotensin-converting enzyme 2 (ACE-2) receptor

Nereida Jiménez de Oya [a,*], Eva Calvo-Pinilla [c], Patricia Mingo-Casas [a], Estela Escribano-Romero [a], Ana-Belén Blázquez [a], Ana Esteban [a], Raúl Fernández-González [b], Eva Pericuesta [b], Pedro J. Sánchez-Cordón [c], Miguel A. Martín-Acebes [a], Alfonso Gutiérrez-Adán [b,1], Juan-Carlos Saiz [a,1]

[a] Departamento de Biotecnología, Instituto Nacional de Investigación y Tecnología Agraria y Alimentaria (INIA-CSIC). Ctra. de La Coruña, km 7, 5, Madrid 28040, Spain
[b] Departamento de Reproducción Animal, INIA-CSIC. Av. Puerta de Hierro, 18, Madrid 28040, Spain
[c] Centro de Investigación en Sanidad Animal, INIA-CSIC. Carretera Algete-El Casar de Talamanca, Km. 8,1, 28130 Valdeolmos, Madrid, Spain

ARTICLE INFO

Keywords:
SARS-CoV-2
ACE2 receptor
Animal models
VOCs
Pathogenesis

ABSTRACT

The emergence of SARS-CoV-2 in 2019 and its rapid spread throughout the world has caused the largest pandemic of our modern era. The zoonotic origin of this pathogen highlights the importance of the One Health concept and the need for a coordinated response to this kind of threats. Since its emergence, the virus has caused >7 million deaths worldwide. However, the animal source for human outbreaks remains unknown. The ability of the virus to jump between hosts is facilitated by the presence of the virus receptor, the highly conserved angiotensin-converting enzyme 2 (ACE2), found in various mammals. Positivity for SARS-CoV-2 has been reported in various species, including domestic animals and livestock, but their potential role in bridging viral transmission to humans is still unknown. Additionally, the virus has evolved over the pandemic, resulting in variants with different impacts on human health. Therefore, suitable animal models are crucial to evaluate the susceptibility of different mammalian species to this pathogen and the adaptability of different variants. In this work, we established a transgenic mouse model that expresses the feline ACE2 protein receptor (cACE2) under the human cytokeratin 18 (K18) gene promoter's control, enabling high expression in epithelial cells, which the virus targets. Using this model, we assessed the susceptibility, pathogenicity, and transmission of SARS-CoV-2 variants. Our results show that the sole expression of the cACE2 receptor in these mice makes them susceptible to SARS-CoV-2 variants from the initial pandemic wave but does not enhance susceptibility to omicron variants. Furthermore, we demonstrated efficient contact transmission of SARS-CoV-2 between transgenic mice that express either the feline or the human ACE2 receptor.

1. Introduction

Severe acute respiratory syndrome coronavirus 2 SARS-CoV-2 belongs to the complex group of coronaviruses encompassing four genera of single-stranded, positive-sense RNA viruses [1,2] responsible for important human and animal diseases. SARS-CoV-2 is a zoonotic pathogen that was presumably transmitted to humans from an unknown mammalian host, although bats have been signaled as the most probable ancestral hosts. The infectivity of the virus in animal cells depends on the existence of the angiotensin-converting enzyme 2 (ACE2), which the virus uses as an entry receptor into the host cell. The spike protein (S) of the virus binds to the cell through its receptor-binding domain (RBD) and is cleaved *via* furin at a polybasic cleavage site, facilitating virus entry and host range [3]. ACE2 is widely distributed among mammals, potentially enabling SARS-CoV-2 to infect several host species. For example, bat coronaviruses related to SARS-CoV-2 can attach to human cells expressing the human ACE2 receptor (hACE2) *via* the RBD, but they lack the furin cleavage region that is involved in mechanisms of pathogenicity in humans [4]. Wild-type mice are not susceptible to early SARS-CoV-2 isolates, however, the expression of hACE2 in transgenic

* Corresponding author.
E-mail address: jdeoya@inia.csic.es (N. Jiménez de Oya).
[1] These authors contributed equally

https://doi.org/10.1016/j.onehlt.2024.100744
Received 20 October 2023; Accepted 26 April 2024
Available online 29 April 2024

mice confers susceptibility to these isolates, confirming the key role of this receptor in viral infectivity and providing a valuable model to study this disease [5,6].

From a One Health perspective, surveillance of SARS-CoV-2 infections in cats was addressed promptly because of their close interaction with humans. Initial studies aimed at detecting viral RNA in domestic cats yielded contradictory results [7–9]. However, a high prevalence of anti-SARS-CoV-2 antibodies, especially in cats from households with COVID-19, was reported [10,11]. Subsequently, in these animals, both natural and experimental infections, along with transmission to unexposed animals in close contact, were documented [12–15]. Nevertheless, infected cats typically do not display clinical signs such as increased body temperature, weight loss, or respiratory distress; instead, they develop a self-limited disease primarily localized to the upper respiratory tract [15].

Although the connection between the cat ACE2 and SARS-CoV-2 has been experimentally confirmed [16], its relevance to *in vivo* infection still needs to be demonstrated. In this study, we have generated transgenic mouse lines expressing either the human or cat ACE2 receptor under the human cytokeratin 18 (K18) gene promoter's control (hACE2 and cACE2, respectively), to assess their susceptibility, pathogenicity, and transmission capacity, thereby evaluating their potential as an experimental animal model.

2. Materials and methods

2.1. Ethics statements

All experimental procedures involving animals were carried out in accordance with the Ethical Committee of Animal Experimentation of INIA-CSIC and by the Division of Animal Protection of the Comunidad de Madrid (PROEX 115.5–21). Animal manipulations were carried out in accordance with the guidelines of Directive 86/609/EEC on the Protection of Animals Used for Experimental and Other Scientific Purposes.

2.2. Generation and characterization of cat ACE2 transgenic mice

Transgenic mice expressing cat ACE2 (cACE2) under the control of the human cytokeratin 18 gene promoter (K18-cACE2) were created by substituting human ACE2 with cACE2 using the pK18-hACE2 plasmid (Fig. 1A) [17]. The K18 segment encompassed the initial 2.5-kb genomic stretch, promoter, and the primary human K18 gene intron. Meanwhile, the K18 3′ section included exon 6, intron 6, exon 7, and the last 300 bp of the human K18 gene's 3′UTR, which contains the K18 poly(A) signal. To enhance translation near the cACE2 start codon and achieve a high degree of epithelial cell-specific expression, we incorporated a translational enhancer (TE) from alfalfa mosaic virus. This addition was previously proven necessary for robust epithelial cell-specific expression. [18]. C57BL/6 mice were used for transgene production, with controlled housing conditions. The transgene construct was excised from the vector by digesting with *HpaI* and *XbaI*, yielding a 6.8 kb DNA fragment. This fragment was purified and microinjected into pronuclear stage embryos. PCR analysis using specific primers (ATCCCTGGCTTTCTATTCATGG/ GCCTGCAATTGACGTTTGACGGT) confirmed the presence of the transgene in the offspring, with founders verified by Sanger sequencing. Four transgenic lines were generated, and mRNA expression of cACE2 in the trachea, lung, and colon was determined by qRT-PCR following already described procedures [18] and primers (GGCTCCTTCTCAGCTTTGCTGC/ GCCTGCAATTGACGTTTGACGGT), for selection of the lines with the best expression. Heterozygotes were utilized in all experiments, with wild-type B6 (WT) mice as negative controls.

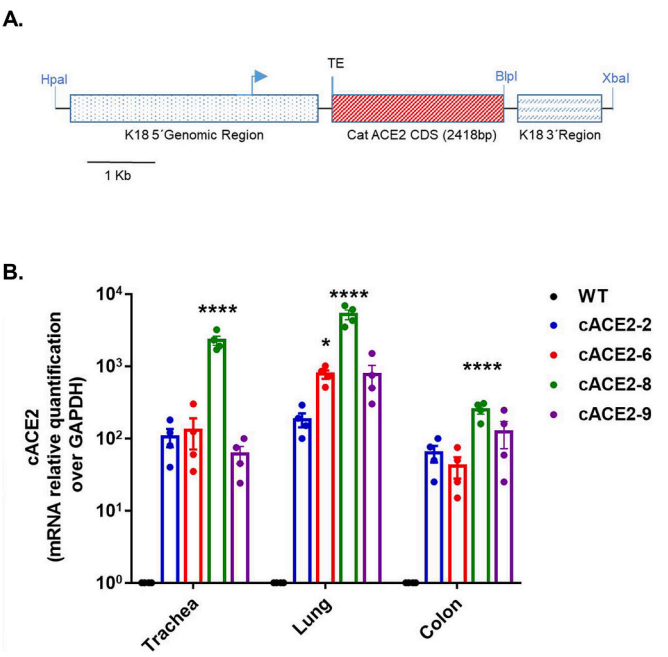

Fig. 1. Generation and characterization of cACE2 mice. (**A**) Schematic view of the expression cassette of plasmid pK18-cACE2 as described [35]. (**B**) Relative quantification of cACE2 mRNA expression in WT and cACE2 transgenic mice from Lines 2, 6, 8, and 9. Transgene expression was calculated relative to GAPDH by q-RT-PCR in six-week-old female mice ($n = 4$ for line). Biological triplicate data for q-RT-PCR are presented as mean ± SEM. Asterisks in the figures denote statistically significant differences $^{**}P < 0.05$.

2.3. Viruses

SARS-CoV-2 isolate hCoV-19/ Spain/SP-VHIR.02, D614G(S) from lineage B.1.610, and lineage BA.1.17 omicron (hCoV-19/Spain/MD-H12O_1620/2021; Gisaid: EPI_ISL_7781198) were propagated in Vero E6 cells (African green monkey kidney epithelial cells, ATCC, CRL-1586) or Vero E6-TMPRSS2 cells, respectively. SARS-CoV-2 D614G was titrated in Vero E6 cells as previously described [19]. Virus titer of omicron was determined using end-point dilutions in 96-well plates of Vero E6 cells according to Spearman and Karber's method and expressed as TCID50.ml–1.

2.4. Mice susceptibility assays

Groups ($n = 12$) of wild-type (WT) C57BL/6, transgenic hACE2 [18], and newly generated cACE2 mice were anesthetized with 5–2% of isoflurane (+0.5–1 l/min) and intranasally (i.n.) inoculated with 50 µl of SARS-CoV-2 D614G(S) (5×10^4 plaque forming units (PFU)/mouse) or the omicron variant (10^4 $TCID_{50}$/mouse). Mice were given food and water *ad libitum* and monitored daily for clinical signs and body weight. At 4 days post-infection (d.p.i.), groups of animals ($n = 6$) were anesthetized and sacrificed. Those mice showing advanced clinical parameters of infection compatible with previously established humanized endpoints were anesthetized and sacrificed by cervical dislocation, as were all the animals at the end of the experiment (15 d.p.i.).

2.5. Mice transmissibility assays

Groups ($n = 6$) of transgenic hACE2 or cACE2 mice were anesthetized, inoculated with SARS-CoV-2 D614G(S), as above, and housed with either uninfected transgenic hACE2 or cACE2 mice (n = 6/group). Blood was recovered at 17 d.p.i. of all surviving animals for serum analysis.

2.6. Viral genomes and cytokine detection

Total RNA was extracted from the right lung of the mice to determine the presence and levels of genomic SARS-CoV-2 RNA and to perform relative quantification of the pro-inflammatory IL-6 and TNF-α cytokines by q-RT-PCR [18].

2.7. Serology

Whole blood was recovered in Microvette® Z: clot activator tubes, let clot for 15 min, and centrifuged at 10000*g* for 5 min. Sera were heat-inactivated (30 min at 56 °C) to detect murine IgGs against the nucleoprotein (N) of SARS-CoV-2 using the Recombivirus™ Mouse Anti-SARS-CoV-2 Virus (COVID-19) Nucleoprotein IgG ELISA kit (ALPHA DIAGNOSTIC).

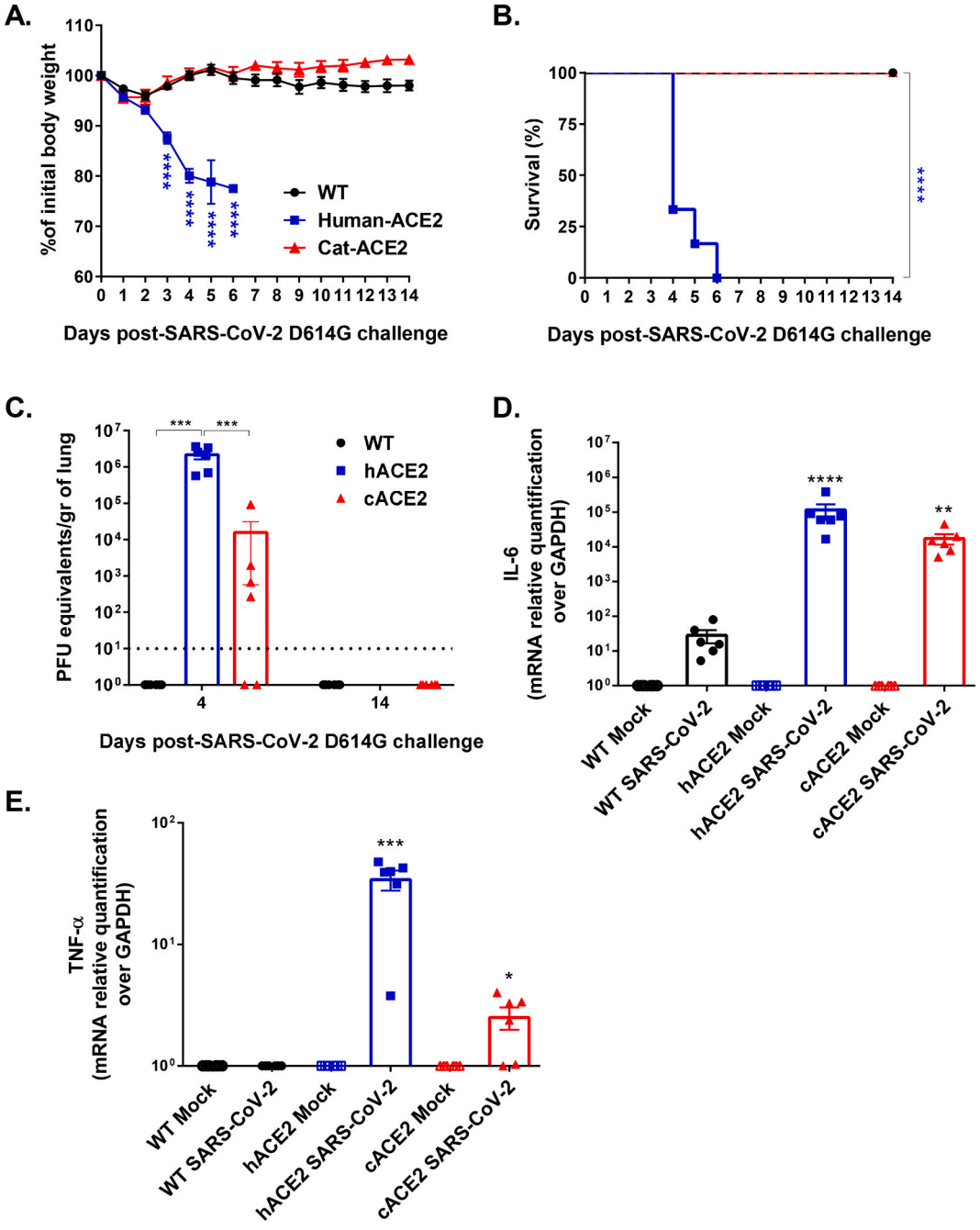

Fig. 2. Susceptibility of cACE2 transgenic mice to SARS-CoV-2 D614G infection. Groups ($n = 12$) of WT, hACE2, or cACE2 mice were intranasally inoculated with 5×10^4 plaque forming units (PFU)/mouse of SARS-CoV-2 D614G. (**A**) Percentage of initial body weight of animals relative to their body weight on day 0. (**B**) Percentage of daily mice survival in each experimental group up to 14 d.p.i. (**C**) Viral genomes expressed as PFU equivalents/g of tissue on mice lungs at days 4 and 14 d.p.i. measured by q-RT-PCR. The dotted line represents the limit of the assay detection. (**D** and **E**) Levels of mRNA of IL-6 (**D**) and TNF-α (**E**) pro-inflammatory cytokines in the lungs of infected and uninfected mice (4 d.p.i.), measured by q-RT-PCR and expressed as a relative quantification using GAPDH as a housekeeping gene and the $2^{-\Delta\Delta Ct}$ method. When applicable, results are expressed as mean ± SEM. Asterisks in the figures denote statistically significant differences *P<0.05, **P<0.01, ***P<0.001, and **** P<0.0001.

2.8. Histopathological study

The left lung lobe of each mouse was fixed by immersion in buffered formalin solution for 48 h. After fixation, samples were processed for histopathological evaluations. The evaluation of possible histopathological lesions and their severity was based on already described parameters of lung inflammation in murine models infected with SARS-CoV-2. [20–22].

2.9. Statistics

GraphPad PRISM 7 (GraphPad Software, La Jolla, CA, USA) was utilized to analyze and represent the data. Kaplan–Meier survival analysis was performed for survival curves. Unpaired two-tailed *t*-test or Mann-Whitney test were done for comparison of parametric or non-parametric two-data sets, respectively. One-way or Two-way ANOVA was used for multiple comparisons of parametric data sets, with pairwise comparison by post-hoc Bonferroni test. Kruskal-Wallis test and Dunn's test were used for multiple comparisons of non-parametric data sets. When applicable, results are expressed as mean ± SEM. Asterisks in the figures denote statistically significant differences *P<0.05, **P<0.01, ***P<0.001, and **** P<0.0001.

3. Results

3.1. Generation of transgenic mice and expression of cat ACE2 in the lines

We produced 4 transgenic mouse lines that express the cat ACE2 protein receptor (cACE2) under the control of the human cytokeratin 18 (K18) gene promoter. Both male and female transgenic mice developed normally and were fertile. The mRNA expression of cat ACE2 in the trachea, lungs, and colon was analyzed. As depicted in Fig. 1B, line 8 showed the highest expression of cACE2 in all analyzed tissues and, was therefore chosen for subsequent experiments, always carrying the transgene in heterozygosity.

3.2. Susceptibility of cat ACE2 transgenic mice to SARS-CoV-2 D614G infection

To explore the relevance of the cat ACE2 receptor for SARS-CoV-2 infection, we tested the susceptibility of cACE2 mice to an isolate from the first infectious wave carrying the D614G mutation, which shares a 99.98% identity with the Wuhan isolate (hCoV-19/Wuhan/WIV04/2019|EPI ISL 402124|2019-12-30) and compared the results with those of hACE2 and WT mice. Upon infection, only hACE2 mice lost weight significantly from day 3 post-infection (p.i.), unlike cACE2 or wild-type (WT) mice that did not (Fig. 2A). Even more, only humanized mice succumbed to the infection, as not a single animal survived by day 6 p.i. (Fig. 2B). However, at 4 days post-infection (d.p.i.), SARS-CoV-2 D614G genomes were detected in the lungs of transgenic mice from both groups, but not in those from the WT. All hACE2 (100%) and 4/6 (66.66%) of the cACE2 were positive, although the titers were significantly lower in the latter (Fig. 2C). No viral genomes were detected in any surviving animal at 14 d.p.i. (Fig. 2C). Furthermore, at 4 d.p.i., both infected transgenic mice, expressing either the human or the cat ACE2 receptor, presented significantly higher values of IL-6 and TNF-α mRNAs (Figs. 2D and E), hallmarks of SARS-CoV-2 pathogenicity in the lungs, compared to infected WT mice. Consistently, histopathological evaluation of lung samples collected on day 4 p.i. revealed significantly higher lung inflammation scores in infected hACE2 and cACE2 mice compared to infected WT mice (Figs. 3A and B). These findings demonstrate that the presence of the cACE2 receptor renders susceptibility to SARS-CoV-2 D614G in the mouse model.

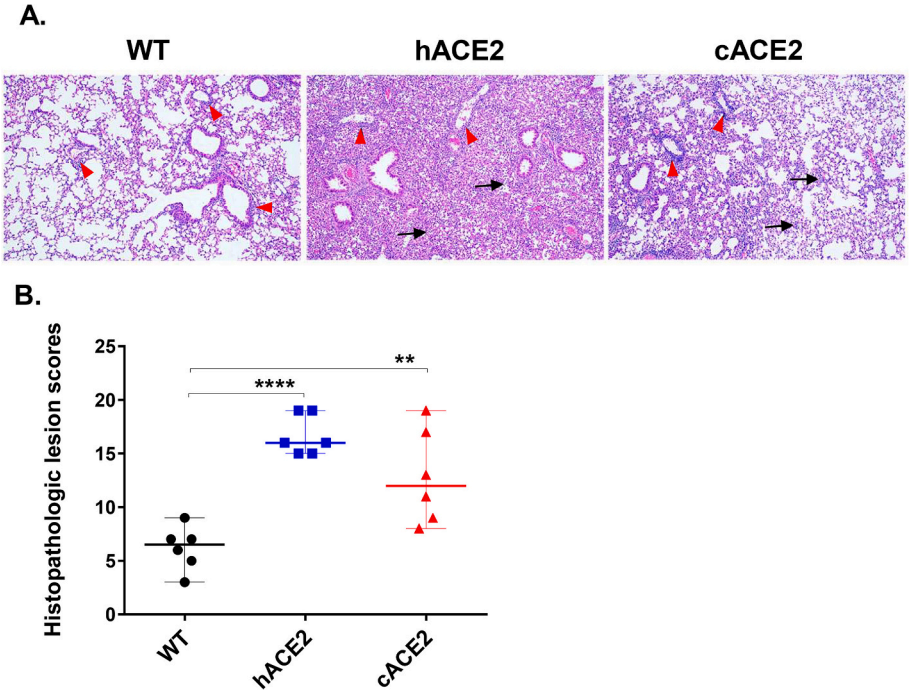

Fig. 3. Histopathological analysis of cACE2 transgenic mice infected with SARS-CoV-2 D614G. Groups ($n = 6$) of WT, hACE2, or cACE2 mice were intranasally inoculated with 5×10^4 plaque forming units (PFU)/mouse of SARS-CoV-2 D614G. (**A**) Representative histopathological images of infected mice lungs at 4 d.p.i. (H&E stain; magnification 10×). Note how lung inflammatory lesions were more severe and extensive in infected hACE2 and cACE2 mice than in infected WT mice. Among lesions highlighted the presence of diffuse septal thickening, perivascular and peribronchiolar mononuclear infiltrates consisting mainly of lymphocytes (red arrowheads) as well as the presence of alveolar mononuclear infiltrates consisting mainly of lymphocytes and macrophages (black arrows). (**B**) Histopathological scores of lesions observed in the lungs of infected mice at 4 d.p.i. When applicable, results are expressed as mean ± SEM. Asterisks in the figures denote statistically significant differences **P<0.01 and **** P<0.0001. (For interpretation of the references to colour in this figure legend, the reader is referred to the web version of this article.)

3.3. Susceptibility of cat ACE2 transgenic mice to SARS-CoV-2 omicron infection

During the pandemic, SARS-CoV-2 has accumulated mutations in the S protein, leading to the emergence of variants of concern (VOCs). In this study, we utilized the omicron variant GISAID EPI_ISL_7781198, which exhibited 15 amino acid changes in the RBD (G339D, S371L, S373P, S375F, K417N, N440K, G446S, S477N, T478K, E484A, Q493K, G496S, Q498R, N501Y, Y505H) compared to the original SARS-CoV-2 [19]. WT mice infected with this omicron variant showed a significant loss of body weight in comparison to both the transgenic humanized mouse model (at days 3 and 4 p.i.), and the mice expressing the cat ACE2 receptor (at day 4 p.i.). On the other hand, humanized transgenic mice showed a significant loss of weight at 7 days p.i. in comparison to the other two experimental groups (Fig. 4A). Survival analysis showed that only hACE2 transgenic mice succumbed to the infection (25% of survival) from day 3 to 7 p.i. (Fig. 4B).

All three groups of mice, including WT and both transgenic mice expressing either the human or the cat ACE2 receptor, were infected by the SARS-CoV-2 omicron variant, as viral genomes were detected in the lungs of mice from all groups at 4 days p.i., albeit with lower titers in mice expressing the cat ACE2 receptor (Fig. 4C). At 15 d.p.i. all mice tested were negative with the exception of one cACE2 mouse in which low, but detectable viral genomes were recorded (Fig. 4C). Pro-inflammatory IL-6 cytokine expression was detected in animals from the three groups, with significantly higher levels in the humanized mice at 4 d.p.i. At 15 d.p.i. transgenic mice expressing either the human or the cat ACE2 receptor presented significantly higher levels of IL-6 expression than WT mice (Fig. 4D). Histopathological analysis of lung samples collected on day 4 p.i. showed significantly higher inflammation scores in WT mice compared to cACE2 mice. In addition, although not statistically significant, lung lesions tended to be more severe in hACE2 than in cACE2 mice (Figs. 5A and B). These results showed that the omicron variant can infect mouse models irrespective of the presence of the WT, the human, or the cat ACE2 receptor and that the presence of the cACE2 receptor does not increase susceptibility to SARS-CoV-2 omicron in the mouse model.

3.4. Contact transmission of SARS-CoV-2 D614G from infected human and cat ACE2 transgenic mice to uninfected human and cat transgenic mice

Considering that cat ACE2 only increased susceptibility to the SARS-CoV-2 D614G isolate, this strain was chosen for transmissibility studies involving contact transmission capacity between the transgenic mouse models. We infected groups ($n = 6$) of hACE2, or cACE2, mice which were then housed for 17 d.p.i. with groups (n = 6) of uninfected hACE2 or cACE2 mice (Fig. 6). With this setup, we were able to study the transmission of the virus *via* contact in human-to-human, human-to-cat, cat-to-cat, and cat-to-human settings. Only experimentally infected

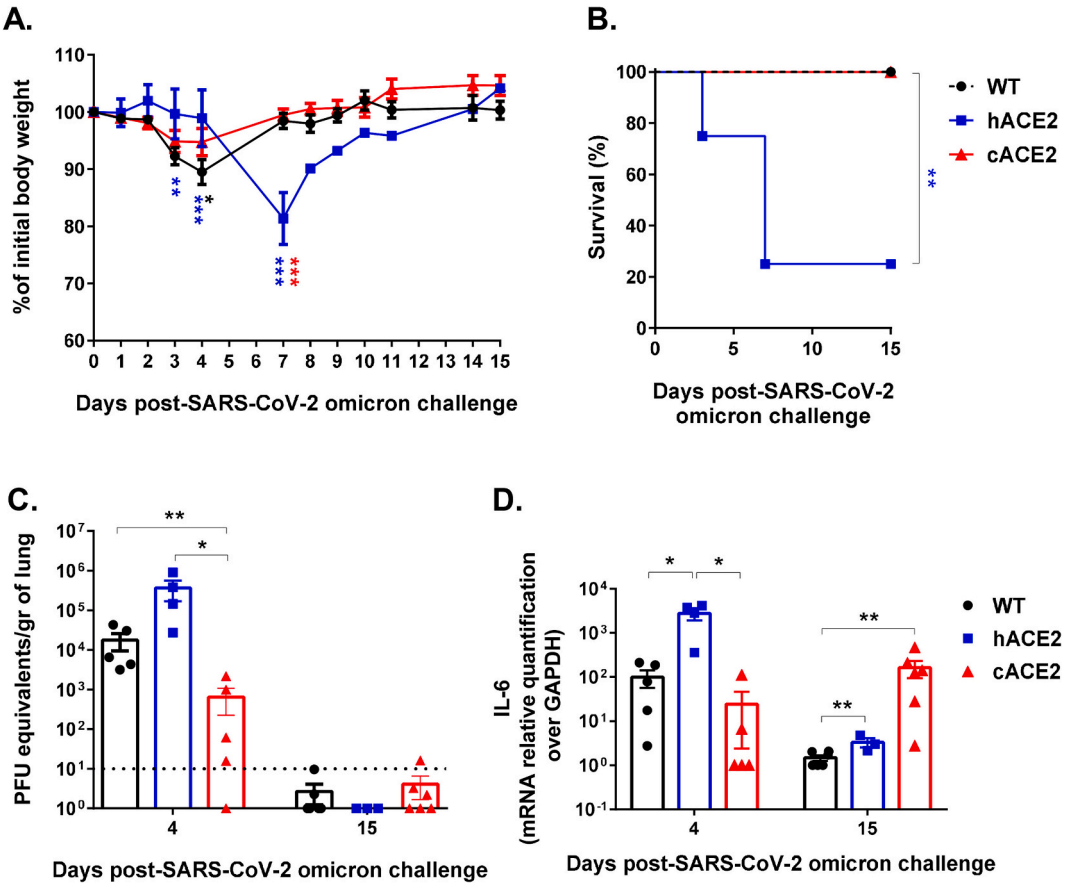

Fig. 4. Susceptibility of cACE2 transgenic mice to SARS-CoV-2 omicron infection. Groups of WT, hACE2, or cACE2, (n = 12/group) were intranasally inoculated with a dose of 10^4 $TCID_{50}$/mouse of SARS-CoV-2 omicron variant. (**A**) Percentage of daily body weight of animals relative to their body weight on day 0. (**B**) Percentage of daily mice survival in each experimental group up to 15 days post-infection. (**C**) Viral genomes expressed as PFU equivalents/g of tissue on mice lungs at days 4 and 15 d.p.i. measured by q-RT-PCR. The dotted line represents the limit of the assay detection. (**D**) Levels of IL-6 mRNA in the lungs of infected mice at 4 and 15 d.p.i. measured by q-RT-PCR and expressed as a relative quantification using GAPDH as a housekeeping gene and the $2^{-\Delta\Delta Ct}$ method. When applicable, results are expressed as mean ± SEM. Asterisks in the figures denote statistically significant differences *P<0.05, **P<0.01, and ***P<0.001. In (**A**) blue, black, and red asterisks represent differences between WT *vs* hACE2, WT *vs* cACE2, and hACE2 *vs* cACE2, respectively. (For interpretation of the references to colour in this figure legend, the reader is referred to the web version of this article.)

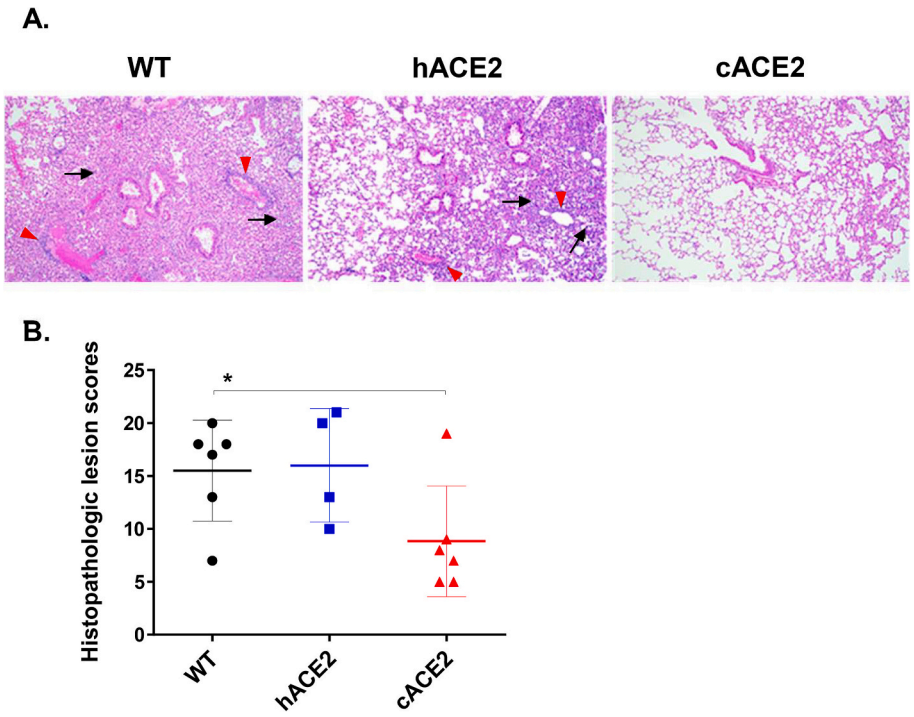

Fig. 5. Histopathological analysis of cACE2 transgenic mice infected with SARS-CoV-2 omicron. Groups of WT, hACE2, or cACE2, (n = 6/group) were intranasally inoculated with a dose of 10^4 $TCID_{50}$/mouse of the SARS-CoV-2 omicron variant. (**A**) Representative histopathological images of infected mice lungs at 4 d.p.i. (H&E stain; magnification 10×). Inflammatory lesions were more severe in WT and hACE2 mice compared to cACE2 mice. Images show the presence of diffuse septal thickening, perivascular and peribronchiolar mononuclear infiltrates mainly constituted by lymphocytes (red arrowheads) as well as the presence of alveolar mononuclear infiltrates mainly constituted by lymphocytes and macrophages (black arrows). (**B**) Histopathological scores of lesions observed in the lungs of infected mice at 4 d.p.i. When applicable, results are expressed as mean ± SEM. Asterisks in the figures denote statistically significant differences *P<0.05. (For interpretation of the references to colour in this figure legend, the reader is referred to the web version of this article.)

hACE2 lost weight significantly (Fig. 6B, C, D, and E). In the "human-to-human" transmission setting, experimentally infected hACE2 succumbed to the infection (survival rate, 16.67%) between days 5 and 6 p.i., as did one contact hACE2 mice at day 8 (survival rate, 83.33%). In the "human-to-cat" setting all experimentally infected humanized transgenic mice died between days 4 and 7 p.i., whereas none of the contact cACE2 mice succumbed to the infection (Figs. 6F, and G). In the "cat-to-cat" and the "cat-to-human" settings, none of the experimentally infected or contact mice died (Figs. 6H, and I). Transmission of the SARS-CoV-2 D614G was confirmed in all groups by the detection of specific IgG antibodies directed against the nucleoprotein of SARS-CoV-2, although with different extents (Fig. 6J). Transmission efficiency was remarkably high in the hACE2 model, with 100% transmission to both hACE2 and cACE2 contact mice. In contrast, transmission from infected transgenic cACE2 animals was less efficient, with transmission rates of 66.66% and 33.33% to cACE2 and hACE2 contact mice, respectively (Fig. 4J). These findings demonstrated a high contact transmission capacity of SARS-CoV-2 D614G between mouse models expressing either the human or the cat ACE2 receptor.

4. Discussion

ACE2 serves as the viral receptor in human cells, but homologous receptors are widespread among other mammals, thereby raising the possibility that these animals could act as new intermediate hosts where the virus can mutate and generate new outbreaks in humans [23–25]. Indeed, natural and experimental infections of SARS-CoV-2 have been reported in at least 18 different domestic and wild animal species [26], with several capable of inter and intra-species virus transmission [27,28]. Natural and experimental infections of cats with SARS-CoV-2 and subsequent transmission to naïve animals in close contact have been reported [12–15]. However, cats generally do not display clinical signs and develop a self-limited disease primarily localized to the upper respiratory tract [14,29–31]. Here, we have used a newly generated line of transgenic mice. Animals were infected with either an isolate (D614G) from the original lineage B.1.610 responsible for the global pandemic, or an omicron isolate (lineage BA.1.17), an attenuated VOC with a high human-to-human transmission potential. Our data demonstrate that the expression of the cat ACE2 receptor alone confers susceptibility to SARS-CoV-2 D614G in the mouse model, albeit to a lesser extent than the human ACE2 receptor. Mice expressing the cat receptor did not exhibit observable clinical signs or succumb to the infection, unlike the humanized model. However, viral RNA was detectable in the lungs of mice expressing the cat ACE2 receptor, albeit at significantly lower levels compared to humanized mice. Furthermore, at four days post-infection, infected mice expressing the cat receptor showed significantly elevated levels of pro-inflammatory interleukins, such as IL-6 and TNF-alpha, in the lungs. These elevations are indicative of the inflammation and tissue damage commonly observed in SARS-CoV-2-infected lungs. Histopathological evaluations also revealed inflammatory lesions in the lungs of infected animals four days post-infection, similar to that observed in humanized mice. These findings align with previous experimental infections of cats, where susceptibility to the infection has been observed, although clinical signs are rare [29,30]. As previously described [32], WT mice that express the murine ACE2 receptor, used as control, did not support SARS-CoV-2 infection belonging to the lineage B.1.610. No clinical signs or viral RNA were detected in WT mice.

All groups of mice (WT, hACE2, and cACE2) were susceptible to infection with the omicron variant, although only hACE2 mice succumbed to the infection (75% of mortality between 3 and 7 d.p.i.). Viral genomes were detected at 4 d.p.i. in all WT and hACE2 mice and, although with significantly lower titers, in 5 of 6 cACE2 mice. Pro-inflammatory cytokine IL-6 levels were detected in mice of all groups at 4 and 15 d.p.i., with significantly higher levels in the humanized

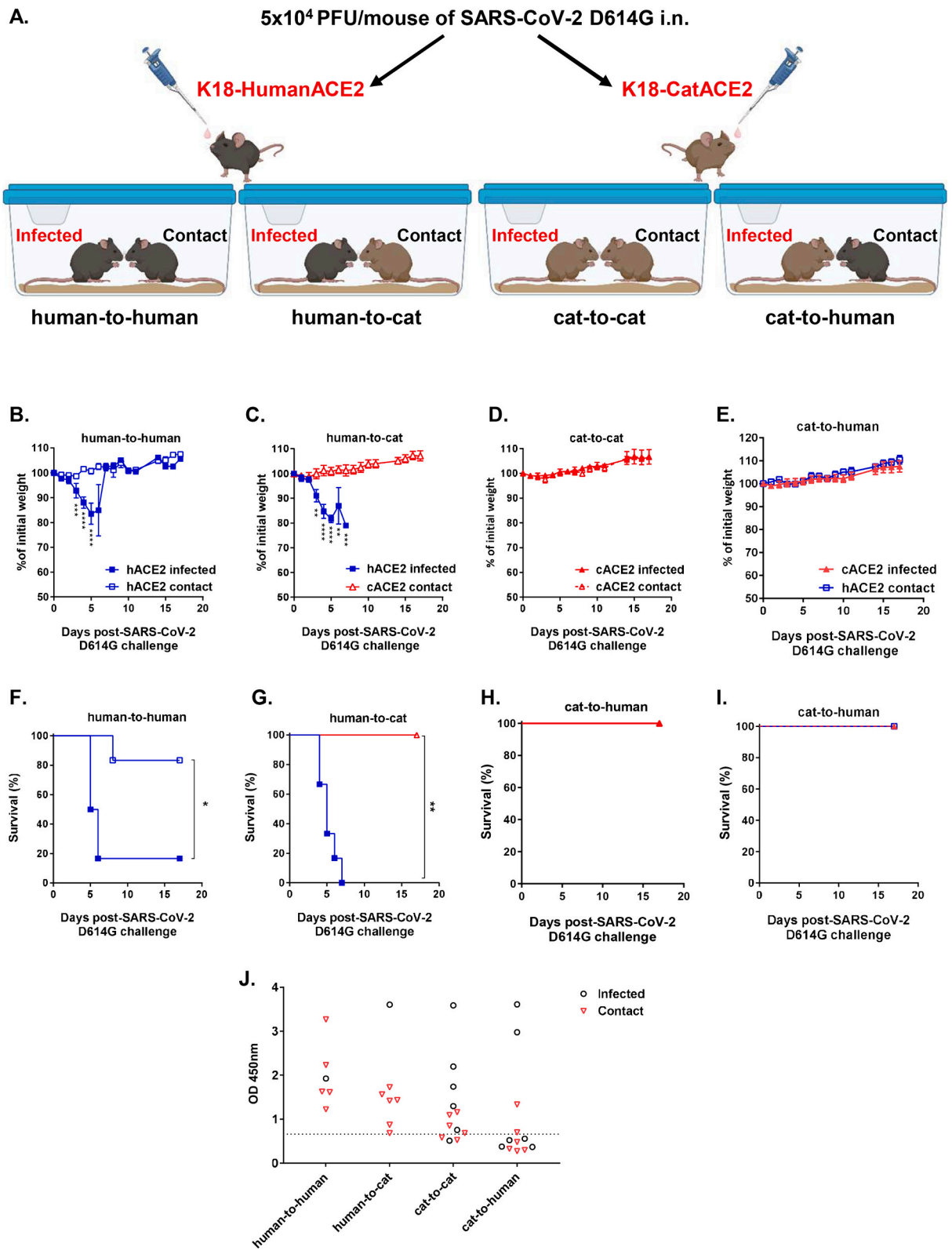

Fig. 6. Contact transmission of SARS-CoV-2 D614G from infected human and cat ACE2 transgenic mice to uninfected human and cat transgenic mice. (**A**) Experimental design. Groups (n = 6) of hACE2 or cACE2 were intranasally inoculated with a dose of 5 × 10^4 plaque forming units (PFU)/mouse of SARS-CoV-2 D614G, and housed for 17 d.p.i. with uninfected hACE2 or cACE2 mice (n = 6/group) to study the transmission of the virus between the different mice-expressing human or cat ACE2 receptor. The figure was created using BioRender.com. (**B, C, D,** and **E**) Percentage of daily body weight of animals relative to their body weight on day 0 before infection in groups in which the experimentally infected mice express the human (**B** and **C**) or the cat (**D** and **E**) ACE2 receptor. (**F, G, H,** and **I**) Percentage of daily mice survival in groups in which the experimentally infected mice express the human (**F** and **G**) or the cat (**H** and **I**) ACE2 receptor up to 17 d.p.i. (**J**) Levels of mouse IgG antibodies against the nucleoprotein of SARS-CoV-2 measured by ELISA. Results are expressed as the average absorbance (OD450) value. The dotted line represents the limit of the assay detection. When applicable, results are expressed as mean ± SEM. Asterisks in the figures denote statistically significant differences *P<0.05, **P<0.01, ***P<0.001, and **** P<0.0001.

model at day 4 p.i. and in both transgenic models at day 15 p.i., compared to WT mice. Additionally, histopathological lesions were observed in mice from all three experimental groups at 4 d.p.i., although statistically significant differences were only recorded between WT and cACE2 mice. Since all three lines of mice used in this study express the murine ACE2 receptor, our data demonstrate that the co-expression of the mouse receptor with the human ACE2 receptor confers susceptibility and pathogenicity to omicron infection. By contrast, co-expression of the cat receptor with the murine receptor does not increase susceptibility to the omicron variant. The susceptibility of both transgenic models was higher to the SARS-CoV-2 D614G variant compared to the omicron variant, confirming previous observations in natural human infections and experimental infections in cats and humanized mice [33,34]. Consequently, due to its higher virulence, the SARS-CoV-2 D614G variant was selected for transmissibility studies. Our findings demonstrate that this strain can be transmitted through direct contact from experimentally infected to uninfected mice, regardless of the expressed receptor by the infected or the contact animals. However, transmission efficiency was greater when the infected animal expresses the human receptor resulting in a 100% transmission rate to both hACE2 and cACE2 mice, compared to a 66.66% transmission rate from infected cACE2 to cACE2 mice and a 33.33% transmission rate to hACE2 mice.

5. Conclusions

We have successfully developed, characterized, and validated a novel line of transgenic mice expressing the cat ACE2 receptor under the control of the human cytokeratin 18 promoter. Our results demonstrate that the expression of cat ACE2 is sufficient to confer susceptibility to SARS-CoV-2 infection in mice to a variant from the first wave of the pandemic, whereas it did not increase susceptibility to an omicron isolate. Therefore, this novel mouse model constitutes a suitable surrogate cat model in laboratory investigations to study the susceptibility, pathogenicity, and transmissibility of potential novel variants of SARS-CoV-2 and other coronaviruses.

Ethical approval and consent to participate

Animal maintenance, handling, and experimental procedures were performed according to the ethical approval information.

Consent for publication

All the authors have read the manuscript and agreed to submit the paper to the journal.

Funding

This study was supported by Fundación BBVA, FBBVA-Eco-Vet-Covid-19 (to AGA), by the Spanish Ministry of Science and Innovation AEI under grants PID2020-119195RJ-I00 (to NJO) and PID2019-105117RR-C21 (to MAMA), by CSIC under grant 202340E181 (to MAMA) and by the European Commission – NextGenerationEU through CSIC's Global Health Platform, PTI Salud Global SGL2103053 (to MAMA). PMC was supported by an FPI fellowship from AEI / 10.13039/501100011033 under grant PRE2020-093374. The funders had no role in study design, data collection, and interpretation, or the decision to submit the work for publication.

Declaration of competing interest

The authors report there are no competing interests to declare.

Data availability

All data generated or analyzed during this study are included in this published article.

Acknowledgments

We thank Dr. Miguel Chillón, Universitat Pompeu Fabra (Barcelona, Spain), and Dr. Rafael Delgado, Hospital Universitario 12 de Octubre (Madrid, Spain) for kindly providing us with SARS-CoV-2 lineage B.1.610, isolate hCoV-19/ Spain/SP-VHIR.02 (D614G(S)), and lineage BA.1.17 VOC omicron variant (hCoV-19/Spain/MD-H12O_1620/2021; Gisaid: EPI_ISL_7781198), respectively.

References

[1] M. Pal, G. Berhanu, C. Desalegn, V. Kandi, Severe acute respiratory syndrome Coronavirus-2 (SARS-CoV-2): an update, Cureus 12 (3) (2020) e7423, https://doi.org/10.7759/cureus.7423.
[2] P. Zhou, X.L. Yang, X.G. Wang, B. Hu, L. Zhang, W. Zhang, et al., A pneumonia outbreak associated with a new coronavirus of probable bat origin, Nature 579 (7798) (2020) 270–273, https://doi.org/10.1038/s41586-020-2012-7.
[3] M. Hoffmann, H. Kleine-Weber, S. Pohlmann, A multibasic cleavage site in the spike protein of SARS-CoV-2 is essential for infection of human lung cells, Mol. Cell 78 (4) (2020) 779–84 e5, https://doi.org/10.1016/j.molcel.2020.04.022.
[4] B.A. Johnson, X. Xie, A.L. Bailey, B. Kalveram, K.G. Lokugamage, A. Muruato, et al., Loss of furin cleavage site attenuates SARS-CoV-2 pathogenesis, Nature 591 (7849) (2021) 293–299, https://doi.org/10.1038/s41586-021-03237-4.
[5] A.C. Knight, S.A. Montgomery, C.A. Fletcher, V.K. Baxter, Mouse models for the study of SARS-CoV-2 infection, Comp. Med. 71 (5) (2021) 383–397, https://doi.org/10.30802/AALAS-CM-21-000031.
[6] T. Pan, R. Chen, X. He, Y. Yuan, X. Deng, R. Li, et al., Infection of wild-type mice by SARS-CoV-2 B.1.351 variant indicates a possible novel cross-species transmission route, Signal Transduct. Target. Ther. 6(1):420 (2021), https://doi.org/10.1038/s41392-021-00848-1.
[7] J. Klaus, E. Zini, K. Hartmann, H. Egberink, A. Kipar, M. Bergmann, et al., SARS-CoV-2 infection in dogs and cats from southern Germany and northern Italy during the first wave of the COVID-19 pandemic, Viruses 13 (8) (2021), https://doi.org/10.3390/v13081453.
[8] V.R. Barrs, M. Peiris, K.W.S. Tam, P.Y.T. Law, C.J. Brackman, To EMW, et al., SARS-CoV-2 in quarantined domestic cats from COVID-19 households or close contacts, Hong Kong, China, Emerg. Infect. Dis. 26 (12) (2020) 3071–3074, https://doi.org/10.3201/eid2612.202786.
[9] S.A. Hamer, A. Pauvolid-Correa, I.B. Zecca, E. Davila, L.D. Auckland, C.M. Roundy, et al., SARS-CoV-2 infections and viral isolations among serially tested cats and dogs in households with infected owners in Texas, USA, Viruses 13 (5) (2021), https://doi.org/10.3390/v13050938.
[10] E.I. Patterson, G. Elia, A. Grassi, A. Giordano, C. Desario, M. Medardo, et al., Evidence of exposure to SARS-CoV-2 in cats and dogs from households in Italy, Nat. Commun. 11 (1) (2020) 6231, https://doi.org/10.1038/s41467-020-20097-0.
[11] G.W. Goryoka, C.M. Cossaboom, R. Gharpure, P. Dawson, C. Tansey, J. Rossow, et al., One health investigation of SARS-CoV-2 infection and Seropositivity among pets in households with confirmed human COVID-19 cases-Utah and Wisconsin, 2020, Viruses 13 (9) (2021), https://doi.org/10.3390/v13091813.
[12] J. Shi, Z. Wen, G. Zhong, H. Yang, C. Wang, B. Huang, et al., Susceptibility of ferrets, cats, dogs, and other domesticated animals to SARS-coronavirus 2, Science 368 (6494) (2020) 1016–1020, https://doi.org/10.1126/science.abb7015.
[13] L. Bao, Z. Song, J. Xue, H. Gao, J. Liu, J. Wang, et al., Susceptibility and attenuated transmissibility of SARS-CoV-2 in domestic cats, J. Infect. Dis. 223 (8) (2021) 1313–1321, https://doi.org/10.1093/infdis/jiab104.
[14] N.N. Gaudreault, J.D. Trujillo, M. Carossino, D.A. Meekins, I. Morozov, D. W. Madden, et al., SARS-CoV-2 infection, disease and transmission in domestic cats, Emerg Microbes Infect. 9 (1) (2020) 2322–2332, https://doi.org/10.1080/22221751.2020.1833687.
[15] P.J. Halfmann, M. Hatta, S. Chiba, T. Maemura, S. Fan, M. Takeda, et al., Transmission of SARS-CoV-2 in domestic cats, N. Engl. J. Med. 383 (6) (2020) 592–594, https://doi.org/10.1056/NEJMc2013400.
[16] L. Wu, Q. Chen, K. Liu, J. Wang, P. Han, Y. Zhang, et al., Broad host range of SARS-CoV-2 and the molecular basis for SARS-CoV-2 binding to cat ACE2, Cell Discov. 6 (2020) 68, https://doi.org/10.1038/s41421-020-00210-9.
[17] A. Gutierrez-Adan, B. Pintado, Effect of flanking matrix attachment regions on the expression of microinjected transgenes during preimplantation development of mouse embryos, Transgenic Res. 9 (2) (2000) 81–89, https://doi.org/10.1023/a:1008926022370.
[18] M. Rodriguez-Pulido, E. Calvo-Pinilla, M. Polo, J.C. Saiz, R. Fernandez-Gonzalez, E. Pericuesta, et al., Non-coding RNAs derived from the foot-and-mouth disease virus genome trigger broad antiviral activity against coronaviruses, Front. Immunol. 14 (2023) 1166725, https://doi.org/10.3389/fimmu.2023.1166725.
[19] J.M. Casasnovas, Y. Margolles, M.A. Noriega, M. Guzman, R. Arranz, R. Melero, et al., Nanobodies protecting from lethal SARS-CoV-2 infection target receptor binding epitopes preserved in virus variants other than omicron, Front. Immunol. 13 (2022) 863831, https://doi.org/10.3389/fimmu.2022.863831.
[20] J. Sun, Z. Zhuang, J. Zheng, K. Li, R.L. Wong, D. Liu, et al., Generation of a broadly useful model for COVID-19 pathogenesis, vaccination, and treatment, Cell 182 (3) (2020) 734–43 e5, https://doi.org/10.1016/j.cell.2020.06.010.

[21] S.H. Sun, Q. Chen, H.J. Gu, G. Yang, Y.X. Wang, X.Y. Huang, et al., A mouse model of SARS-CoV-2 infection and pathogenesis, Cell Host Microbe 28 (1) (2020) 124–33 e4, https://doi.org/10.1016/j.chom.2020.05.020.
[22] P. Perez, D. Astorgano, G. Albericio, S. Flores, P.J. Sanchez-Cordon, J. Luczkowiak, et al., Intranasal administration of a single dose of MVA-based vaccine candidates against COVID-19 induced local and systemic immune responses and protects mice from a lethal SARS-CoV-2 infection, Front. Immunol. 13 (2022) 995235, https://doi.org/10.3389/fimmu.2022.995235.
[23] Z. Liu, X. Xiao, X. Wei, J. Li, J. Yang, H. Tan, et al., Composition and divergence of coronavirus spike proteins and host ACE2 receptors predict potential intermediate hosts of SARS-CoV-2, J. Med. Virol. 92 (6) (2020) 595–601, https://doi.org/10.1002/jmv.25726.
[24] R. Li, S. Qiao, G. Zhang, Analysis of angiotensin-converting enzyme 2 (ACE2) from different species sheds some light on cross-species receptor usage of a novel coronavirus 2019-nCoV, J. Inf. Secur. 80 (4) (2020) 469–496, https://doi.org/10.1016/j.jinf.2020.02.013.
[25] Y. Liu, G. Hu, Y. Wang, W. Ren, X. Zhao, F. Ji, et al., Functional and genetic analysis of viral receptor ACE2 orthologs reveals a broad potential host range of SARS-CoV-2, Proc. Natl. Acad. Sci. USA 118 (12) (2021), https://doi.org/10.1073/pnas.2025373118.
[26] S. Cui, Y. Liu, J. Zhao, X. Peng, G. Lu, W. Shi, et al., An updated review on SARS-CoV-2 infection in animals, Viruses 14 (7) (2022), https://doi.org/10.3390/v14071527.
[27] V.L. Hale, P.M. Dennis, D.S. McBride, J.M. Nolting, C. Madden, D. Huey, et al., SARS-CoV-2 infection in free-ranging white-tailed deer, Nature 602 (7897) (2022) 481–486, https://doi.org/10.1038/s41586-021-04353-x.
[28] J.F. Chan, A.J. Zhang, S. Yuan, V.K. Poon, C.C. Chan, A.C. Lee, et al., Simulation of the clinical and pathological manifestations of coronavirus disease 2019 (COVID-19) in a Golden Syrian Hamster model: implications for disease pathogenesis and transmissibility, Clin. Infect. Dis. 71 (9) (2020) 2428–2446, https://doi.org/10.1093/cid/ciaa325.
[29] D.A. Meekins, N.N. Gaudreault, J.A. Richt, Natural and experimental SARS-CoV-2 infection in domestic and wild animals, Viruses 13 (10) (2021), https://doi.org/10.3390/v13101993.
[30] A.M. Bosco-Lauth, A.E. Hartwig, S.M. Porter, P.W. Gordy, M. Nehring, A.D. Byas, et al., Experimental infection of domestic dogs and cats with SARS-CoV-2: pathogenesis, transmission, and response to reexposure in cats, Proc. Natl. Acad. Sci. USA 117 (42) (2020) 26382–26388, https://doi.org/10.1073/pnas.2013102117.
[31] N. Kruger, C. Rocha, S. Runft, J. Kruger, I. Farber, F. Armando, et al., The upper respiratory tract of felids is highly susceptible to SARS-CoV-2 infection, Int. J. Mol. Sci. 22 (19) (2021), https://doi.org/10.3390/ijms221910636.
[32] L. Bao, W. Deng, B. Huang, H. Gao, J. Liu, L. Ren, et al., The pathogenicity of SARS-CoV-2 in hACE2 transgenic mice, Nature 583 (7818) (2020) 830–833, https://doi.org/10.1038/s41586-020-2312-y.
[33] M. Martins, G.M. do Nascimento, M. Nooruzzaman, F. Yuan, C. Chen, L.C. Caserta, et al., The omicron variant BA.1.1 presents a lower pathogenicity than B.1 D614G and Delta variants in a feline model of SARS-CoV-2 infection, J. Virol. 96 (17) (2022) e0096122, https://doi.org/10.1128/jvi.00961-22.
[34] F. Tarres-Freixas, B. Trinite, A. Pons-Grifols, M. Romero-Durana, E. Riveira-Munoz, C. Avila-Nieto, et al., Heterogeneous infectivity and pathogenesis of SARS-CoV-2 variants Beta, Delta and omicron in transgenic K18-hACE2 and wildtype mice, Front. Microbiol. 13 (2022) 840757, https://doi.org/10.3389/fmicb.2022.840757.
[35] P.B. McCray Jr., L. Pewe, C. Wohlford-Lenane, M. Hickey, L. Manzel, L. Shi, et al., Lethal infection of K18-hACE2 mice infected with severe acute respiratory syndrome coronavirus, J. Virol. 81 (2) (2007) 813–821, https://doi.org/10.1128/JVI.02012-06.